BIOLOGY OF REPRODUCTION **85,** 575–583 (2011)
Published online before print 25 May 2011.
DOI 10.1095/biolreprod.111.091710

Absence of MSY2 in Mouse Oocytes Perturbs Oocyte Growth and Maturation, RNA Stability, and the Transcriptome[1]

Sergey Medvedev, Hua Pan, and Richard M. Schultz[2]

Department of Biology, University of Pennsylvania, Philadelphia, Pennsylvania

ABSTRACT

Messenger RNA is remarkably stable during oocyte growth, thus enabling mRNAs to accumulate during the growth phase and thereby provide mRNAs that support early embryonic development. MSY2, a germ cell-specific RNA-binding protein, is implicated in regulating mRNA stability. MSY2 is essential for development because female *Msy2*$^{-/-}$ mice are infertile. We describe here the characterization of *Msy2*$^{-/-}$ oocytes. Mutant oocytes grow more slowly during the first wave of folliculogenesis, and maturation to and arrest at metaphase II is severely compromised because of aberrant spindle formation and chromosome congression. Consistent with MSY2 conferring mRNA stability is that the amount of poly(A)-containing RNA is reduced by ~25% in mutant oocytes. Stability of an exogenous mRNA injected into mutant oocytes is lower than when compared to their wild-type counterparts, and moreover, expression of wild-type MSY2 in mutant oocytes increases mRNA stability, whereas injection of a mutant form of MSY2 not capable of binding RNA does not. Transcription quiescence that normally occurs during the course of oocyte growth is not observed in mutant oocytes, and the transcriptome of mutant oocytes is markedly perturbed. These results, and those of previous studies, strongly implicate a central role of MSY2 in regulating mRNA stability.

gene expression, histone modifications, meiotic maturation, mRNA stability, oocyte development

INTRODUCTION

Oocyte development is characterized by cell growth in the absence of cell division; oocytes grow while arrested in the first meiotic prophase. In mouse, the first wave of oocyte development takes 22–24 days in most strains and oocyte volume increases by 200–250-fold [1]. During this time, mRNAs are remarkably stable, exhibiting a half-life of ~2 wk [2–5]. Presumably this stability enables oocytes to accumulate mRNAs that will constitute the maternal dowry that drives and supports early preimplantation development, at least until the time of zygotic genome activation. A transition from mRNA stability to instability initiates with resumption of meiosis, in which the amount of poly(A) RNA decreases from 80 pg per oocyte to ~50 pg [6]. Messenger RNA degradation continues during the one-cell and two-cell stages, reaching a nadir of about 10 pg of mRNA in a two-cell embryo [7]. The major phase of zygotic genome activation occurs during the two-cell stage and results in a dramatic reprogramming of gene expression, as well as mRNA accumulation [8].

In female mice, *Msy2* encodes an oocyte-specific RNA-binding protein that comprises about 2% of total oocyte protein [9]. In contrast to male germ cells, in which MSY2 is soluble, about 70% of oocyte MSY2 is retained following membrane permeabilization that releases at least 70% of total oocyte protein [10]. Following fertilization, the amounts of *Msy2* mRNA and MSY2 protein decrease, such that little MSY2 protein is detected in two-cell embryos [9].

In oocytes, MSY2 likely serves a role of regulating global stability of mRNA. Transgenic RNAi-mediated reduction of oocyte *Msy2* transcripts results in development of oocytes that contain about 20% less mRNA and fail to mature correctly, having a wide spectrum of deficiencies in spindle formation [11]. Deletion of the *Msy2* gene results in females that are sterile [12]. In 21-day-old mutant mice, ovarian follicle number and progression are reduced, whereas in adult mutant females, oocyte loss increases, anovulation is observed, and multiple oocyte and follicle defects are seen.

CDC2A-mediated phosphorylation of MSY2 triggers the transition from mRNA stability to instability [13]. In particular, overexpressing a nonphosphorylatable form of MSY2 inhibits the maturation-associated decrease in oocyte mRNAs, whereas overexpressing a putative constitutively active form triggers mRNA degradation in the absence of an increase in CDC2A activity. Messenger RNA degradation appears because of an increase in mRNA accessibility to the RNA degradation machinery, because mRNAs in oocytes overexpressing the constitutively active form of MSY2 are far more sensitive to degradation by exogenous RNase when compared to controls [13].

We report here a cellular and molecular characterization of *Msy2*$^{-/-}$ oocytes. Growth of mutant oocytes during the first wave of folliculogenesis is slightly retarded. Null oocytes also contain ~25% less total poly(A)-containing mRNA, but there is no difference in the fraction that is associated with the Triton X-100 (TX-100)-insoluble fraction when compared to wild-type oocytes. Messenger RNA stability of an exogenous reporter mRNA is reduced in *Msy2*$^{-/-}$ oocytes, and expression of MSY2, but not a mutant form unable to bind RNA, restores stability of the reporter mRNA. Transcript profiling reveals that the relative abundance of at least two thirds of transcripts expressed in mutant oocytes is perturbed. In contrast to wild-type oocytes, cumulus cells are loosely attached to mutant oocytes, which do not undergo the nonsurrounded nucleolus (NSN) to surrounded nucleolus (SN) change in DNA configuration and remain transcriptionally active.

[1]Supported by a grant from the National Institutes of Health (HD022681) to R.M.S.
[2]Correspondence: Richard M. Schultz, Department of Biology, University of Pennsylvania, 433 South University Avenue, Philadelphia, PA 19104-6018. FAX: 215 898 8780; e-mail: rschultz@sas.upenn.edu

Received: 14 February 2011.
First decision: 22 April 2011.
Accepted: 16 May 2011.

eISSN: 1529-7268 http://www.biolreprod.org
ISSN: 0006-3363

MATERIALS AND METHODS

Oocyte and Embryo Collection and Culture

Intercrosses of *Msy2*$^{+/-}$ male and female mice were used to produce *Msy2*$^{-/-}$ females. Germinal vesicle (GV)-intact full-grown oocytes were collected from the ovaries of equine chorionic gonadotropin (eCG)-primed 22-, 24-, and 27-day-old mice 44 h following injection; no hormonal stimulation was used to collect oocytes from the ovaries of 16-, 18-, 19-, and 20-day mice. Oocytes were either allowed to mature in vitro in CZB medium [14] or incubated in the presence of 2.5 μM milrinone (Sigma) to inhibit germinal vesicle breakdown (GVBD) [15]. To produce in vivo-matured oocytes, mice were injected with 5 IU eCG and then with 5 IU human chorionic gonadotropin (hCG) 44 h later; ovulated eggs were harvested from oviducts. Eight-cell embryos were harvested 64 h after hCG injection and mating to 6-wk-old CF1 male mice. All animal experiments were approved by the University of Pennsylvania Institutional Animal Use and Care Committee and were consistent with National Institutes of Health guidelines.

Measurement of Oocyte Size

Oocyte diameter was measured using photo-images of freshly isolated, granulosa/cumulus cell-free oocytes. The long and short diameters were measured, excluding the zona pellucida, for each oocyte using the integrated measuring tools in NIH Image J software (National Institutes of Health) after calibration with a scale marker. The two measurements were averaged and expressed as the diameter of the oocyte. The diameter values for oocyte groups and difference in diameter between *Msy2*$^{-/-}$ and wild-type oocytes were calculated using Prism 4 software (Graph Pad Software Inc.). The distribution of oocyte diameters was generated using Smith's Statistical Package, available at http://www.economics.pomona.edu/StatSite/SSP.html.

TX-100 Treatment and mRNA Purification and Quantification

The TX-100-insoluble fraction was generated as previously described [10]. Briefly, GV oocytes or eight-cell embryos were treated with 0.1% TX-100 containing 100 mM KCl, 5 mM $MgCl_2$, 3 mM ethylene glycol tetraacetic acid, 20 mM Hepes, pH 6.8, and 1% bovine serum albumin (BSA) (intracellular buffer [ICB]) for 10 min at room temperature followed by three washes with ICB.

Poly(A)-containing mRNA from oocytes, eight-cell embryos, or 3T3 cells was purified using a Dynabeads mRNA Direct kit (Dynal A.S.) according to the manufacturer's instructions, followed by quantification using RiboGreen fluorescent dye with a GloMax-Multi Jr Fluorometer system (Turner Biosystems, Inc.).

DNA Constructs and cRNA Synthesis

A construct encoding wild-type *Msy2* (MSY2-EGFP-pXT7) has been described [10]. To produce a non-RNA binding form of MSY, the RNP motif in the CSD of MSY2 (i.e., residues Y109, F111, and D116 and 120) were mutated to A using a single-stranded Phusion mutagenesis protocol (BioLabs). Mutagenic primers were: forward, AGG AAT GCC ACC AAG GAG GCC GTC TTT G; reverse, GTT GAT GGC TCC GGC ACC ATT CCG. The resulting MSY2A construct corresponded to the PM3 construct described previously [10]. All MSY2 constructs have an enhanced green fluorescent protein (EGFP) epitope tag at the carboxyl terminus to monitor protein expression. Both MSY2 and MSY2A constructs were linearized with *Sac1*. Plasmid pIVT-EGFP-N1 was linearized by *Nde1*. Plasmid phRL_SV40 (Promega) was linearized with *Not1*. All constructs were in vitro transcribed using the mMESSAGE mMACHINE T7 kit (Ambion). Complementary RNA from MSY2, MSY2A, and PIVT-N-EGFP was resuspended at a concentration of 2 μg/μl, and cRNA from phRL_SV40 was resuspended at a concentration of 0.02 μg/μl in 10 mM Tris-HCl, pH 7.5, 1 mM EDTA, and stored at −80°C prior to use for microinjection.

In the *Renilla* luciferase rescue experiment, full-grown oocytes were microinjected with ~10 pl of mixture of *Msy2* and *RL* mRNAs, *Msy2A* and *RL* mRNAs, or *Egfp* and *RL* mRNAs, and then incubated overnight in CZB supplemented with 200 μM 3-isobutyl-1-methyl xanthine to maintain meiotic arrest. Microinjection was performed as previously described [16]. Oocytes were briefly examined for EGFP fluorescence using a conventional UV microscope and then harvested and stored at −80°C until use for the luciferase assay.

Luciferase Assay

Renilla luciferase activity was assayed in individual oocytes using the Dual Luciferase Reporter Assay kit (Promega) according to the manufacturer's instructions. Relative light units (RLU) produced on the Monolight 2010 luminometer (Analytical Luminescence Lab) were measured over a period of 20 sec. For each data point the mean value of 10–15 oocytes was used.

In Vitro Transcription Assay

The transcriptional activity in *Msy2*$^{-/-}$ and *Msy2*$^{+/+}$ GV oocytes was determined after 5-bromo uridine triphosphate (Br-UTP; Sigma) incorporation into plasma membrane-permeabilized oocytes essentially as described [17], except that the basic PBS buffer was supplemented with 0.2% polyvinylpyrrolidone (PVP) to reduce the oocyte stickiness. The incorporated Br-UTP was detected with 6 μg/ml anti-BrdU antibody (immunoglobulin G [IgG]; Roche) as the primary antibody and 20 μg/ml fluorescein isothiocyanate-conjugated goat anti-mouse (IgG; SouthernBiotech) as the secondary antibody. TO-PRO3 diluted (1:250) in mount medium was used as a chromatin-specific dye. Nuclear localized fluorescence as an indicator of the transcriptional activity was detected on a Leica TCS SP laser-scanning confocal microscope. Image J software was used to quantify transcriptional activity. Each experimental group included 10–20 oocytes and the experiments were done at least in a triplicate.

Immunocytochemistry

For the immunocytochemical detection of histones, oocytes were fixed in PBS containing 2.5% paraformaldehyde for 20 min at room temperature followed by permeabilization for 10 min in 0.2% TX-100 in PBS. After extensive washing in PBS supplemented with 0.2% PVP (PVP-PBS), oocytes were then incubated overnight with the primary antibody diluted 1:200 in PVP-PBS. The primary antibodies were polyclonal antibodies against hyperacetylated histone H4 (Upstate Biotechnology) and histone H3 trimethylated on K4 (Cell Signaling), monoclonal antibody against histone H3 acetylated on K9 (Upstate Biotechnology), and a polyclonal antibody against RNA pol II CTD phospho Ser5 (Active Motif). Following four 10-min washes in PVP-PBS, the oocytes were incubated for 60 min with the secondary antibody conjugated with Cy5. The cells were then washed three times, 10 min per wash, in PVP-PBS, followed by a 10-min incubation with Sytox Green diluted 1:5000 in PVP-PBS prior to mounting in Vectashield.

To stain the spindle, cells were fixed in PBS containing 3.7% paraformaldehyde for 20 min at room temperature, permeabilized for 10 min in 0.2% TX-100 in PBS, and then, after three 10-min washes in blocking buffer (0.1% BSA, 0.01% Tween-20 in PBS), the cells were incubated for 60 min with a β-tubulin (1:50) antibody (Sigma). After cells were washed three times for 10 min each in blocking buffer, they were then incubated for 60 min with an Alexa 488-conjugated (Molecular Probes) secondary antibody. The cells were again washed three times, 10 min each time, in blocking buffer prior to mounting in Vectashield containing TO-PRO3 (1:250). Fluorescence was detected using a Leica TCS SP laser-scanning confocal microscope. NIH Image J software was used to quantify the intensity of fluorescence. Each experimental group included 10–20 oocytes and the experiments were done at least in triplicate.

Immunoblotting

Proteins were fractionated in a 10% SDS-PAGE gel and transferred to an Immobilon P membrane (Millipore) using semidry transfer. Membranes were processed and developed as previously described [10]. A β-tubulin (1:50) antibody was used at a 1:2000 dilution. Quantification of signals was performed using Image J software.

Messenger RNA Microarray Analysis

RNA from 20 GV-intact oocytes was extracted and amplified, and equal aliquots of total RNA from each of three *Msy2*$^{-/-}$ and three *Msy2*$^{+/+}$ mice (22-day-old, eCG-primed) were converted to biotinylated cRNA as described previously [18]. All RNA specimens were quantified and checked for quality before further manipulation (Supplemental Table S1; all Supplemental Data are available online at www.biolreprod.org). Seventeen micrograms of fragmented cRNA was hybridized (Penn Microarray Facility) with MOE430 v2 GeneChips, which covers 45 000 transcripts and variants, and processed according to the Affymetrix instructions. Data were normalized by the median per gene and per array using GeneSpring v7. Normalized data were then filtered for those called ''absent'' and ''present.'' Genes whose expression was significantly changed in the oocytes from *Msy2*$^{-/-}$ females compared to the control were identified by Significance Analysis of Microarrays (fold change <2.0 for down-regulated and >2.0 for up-regulated; q value < 0.02; and detection probability greater than 0.95 in all samples) or by one-way ANOVA analysis (false discovery rate $<5\%$) and annotated in GeneSpring. The statistically significant gene lists obtained by ANOVA were imported into

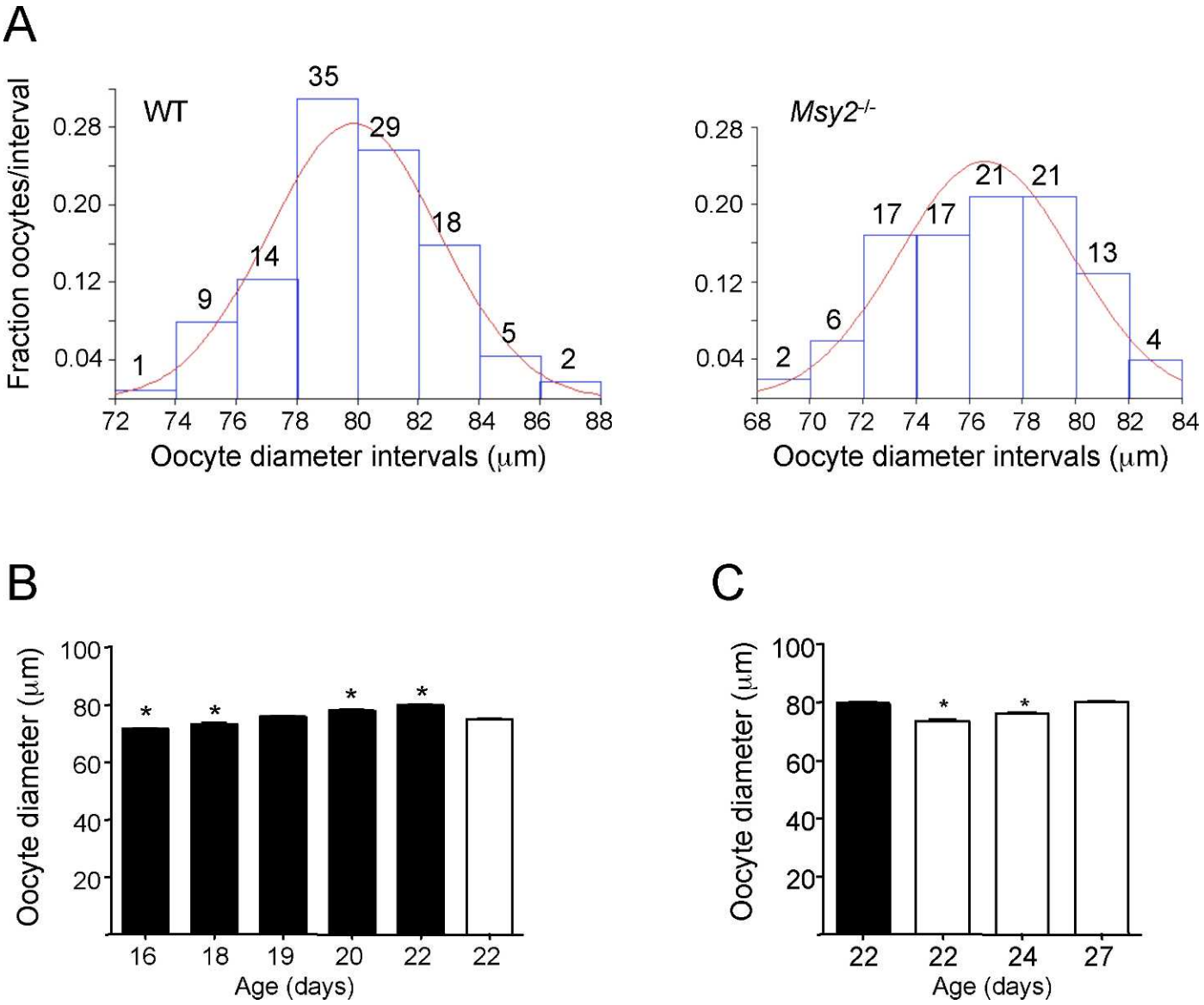

FIG. 1. Distribution of oocyte diameter and growth rates of *Msy2*$^{-/-}$ and wild-type oocytes. **A**) Distribution of wild-type (WT) and *Msy2*$^{-/-}$ oocytes in 2-μm intervals. The numbers above the bars are the number of oocytes. **B**) Increase in oocyte diameter as function of age during first wave of folliculogenesis. Solid bars, wild-type oocytes; open bar, *Msy2*$^{-/-}$ oocytes. The experiment was conducted three times and the data are expressed as the mean ± SEM; >100 oocytes were analyzed at each stage. *$P < 0.001$. **C**) Increase in oocyte diameter as a function of age beyond 22 days of age. Solid bar, wild-type oocytes; open bars, *Msy2*$^{-/-}$ oocytes. The experiment was conducted three times and the data are expressed as mean ± SEM; >95 oocytes were analyzed at each stage. *$P < 0.0001$.

DAVID software (http://david.abcc.ncifcrf.gov) to test for overrepresentation of biological processes in knockout vs. wild-type samples. Hierarchical clustering of samples and gene expression values based on similarities of expression values was performed using the average linkage method.

RESULTS

Morphological Characteristics of Oocytes Obtained from Msy2$^{-/-}$ *Mice*

We focused our attention on characterizing oocyte development during the first wave of folliculogenesis in *Msy2*$^{-/-}$ mice because the pronounced decrease in folliculogenesis observed in cycling mice is not observed during the first wave [12]. Significantly fewer oocytes were obtained from ovaries of 22-day-old mutant mice when compared to wild-type (70 ± 2 vs. 95 ± 3 oocytes/mouse, respectively, $P < 0.0001$). Furthermore, mutant oocytes were slightly smaller in diameter (76.6 ± 0.3 μm, mean ± SEM) than wild-type oocytes (79.9 ± 0.3 μm, mean ± SEM, $P < 0.001$) (Fig. 1A), which translates to a reduction in volume of ~10%. The average oocyte diameter obtained from 22-day-old mutant mice corresponded to the size from oocytes obtained from wild-type mice 19 days of age (Fig. 1B). Oocytes present in mutant mice, however, continued to grow and by day 27 reached an average diameter equal to that of oocytes obtained from wild-type mice 22 days of age (Fig. 1C). Consistent with the reduced number of oocytes isolated from ovaries of mutant mice was the reduced size of their ovaries (Supplemental Fig. S1), which exhibited continued growth and reached the size of wild-type ovaries by 30 days of age (Supplemental Fig. S2). Failure to observe any evidence of ovulation in mutant mice is consistent with the absence of any sign of preovulatory follicle formation (Supplemental Fig. S1).

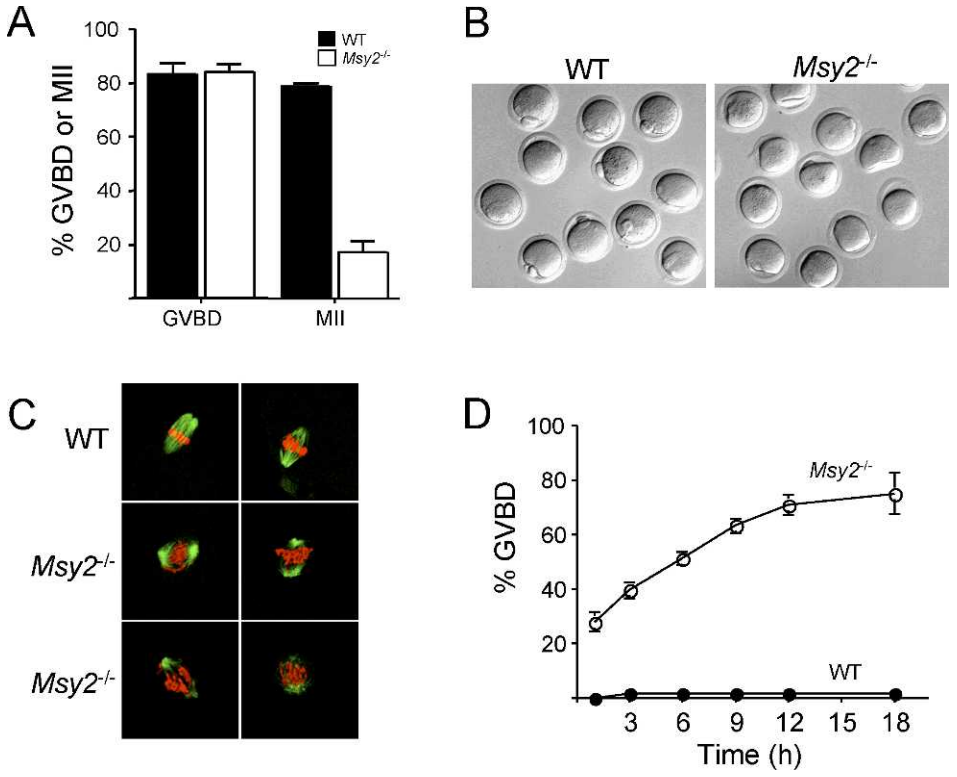

FIG. 2. Maturation properties of *Msy2*$^{-/-}$ oocytes. **A**) Incidence of GVBD and maturation to and arrest at MII following maturation in vitro. Maturation to and arrest at MII was assessed by detecting the presence of a polar body (PB). The experiment was performed six times and the data are expressed as mean ± SEM. Between 50 and 120 oocytes were examined in each group for each experiment. **B**) Photomicrographs of representative wild-type and *Msy2*$^{-/-}$ oocytes matured in vitro. Note presence of PB in wild-type but frequent absence in mutant oocytes. Original magnification ×200. **C**) Immunocytochemical detection of spindles and DNA in wild-type and *Msy2*$^{-/-}$ oocytes matured in vitro. Green, tubulin; red, DNA. Note that compared to wild-type oocytes that exhibit a well-defined spindle with chromosomes tightly along a metaphase plate, mutant oocytes display a variety of abnormal phenotypes. The experiment was performed three times and a total of 43 wild-type and 57 mutant oocytes were analyzed. Original magnification ×400. **D**) Kinetics of maturation of wild-type and *Msy2*$^{-/-}$ oocytes in the presence of 1 μM milrinone. The experiment was performed three times and the data are expressed as mean ± SEM; at least 50 oocytes in each group were used for each experiment.

When matured in vitro, mutant and wild-type oocytes underwent GVBD at the same incidence, but development to and arrest at metaphase II (MII) was dramatically reduced for mutant oocytes (Fig. 2, A and B), the likely basis being dramatic deficiencies in spindle formation and chromosome congression (Fig. 2C). These deficiencies were anticipated because they were observed following transgenic RNAi-mediated targeting of *Msy2* [11]. Unexpectedly, we noted that 1 μM of the phosphodiesterase (PDE) 3A inhibitor milrinone [15], which inhibits the maturation-associated decrease in cAMP that triggers GVBD [19], was not able to maintain effectively meiotic arrest in *Msy2*$^{-/-}$ oocytes in vitro (Fig. 2D); inhibition of maturation was observed when 2.5 μM milrinone was used (data not shown).

RNA Stability in Msy2$^{-/-}$ *Oocytes*

We previously reported that transgenic RNAi-mediated targeting of *Msy2* that results in a decrease in the amount of MSY2 by at least 60% also results in an ~20% decrease in the amount of total poly(A)-containing RNA [11]. We noted a similar reduction in the total amount of poly(A)-containing RNA in *Msy2*$^{-/-}$-deficient oocytes, which contain no detectable MSY2 protein (53.9 ± 1.9 pg/mutant oocyte vs. 70.7 ± 2.0 pg/wild-type oocyte; $P < 0.0001$). The amount of poly(A)-RNA reported here for wild-type oocytes is in agreement with the previous reported value of 80 pg [20].

About 70%–80% of the poly(A)-containing mRNA is present in an insoluble fraction following membrane permeabilization with TX-100 under conditions that release >70% of soluble oocyte protein [10]. A similar amount of MSY2 also resides in this fraction following TX-100, but is released into the soluble fraction following RNase treatment, i.e., integrity of the RNA is essential for localization of MSY2 to this fraction [10]. A formal possibility is that RNA that associates with MSY2 becomes localized to this fraction and that this localization confers increased mRNA stability. Such a scenario was highly unlikely because similar amounts of poly(A)-containing RNA were present in the TX-100-insoluble fraction in wild-type and mutant oocytes (Fig. 3). Furthermore, comparable amounts of poly(A)-containing RNA were present in the TX-100-insoluble fraction in eight-cell embryos and 3T3 cells, neither of which contain MSY2 (Fig. 3). Taken together, these results suggest that although binding of MSY2 to RNA confers RNA stability, MSY2 binding is not required to localize mRNA to the TX-100-insoluble fraction.

Further evidence that MSY2-binding stabilizes mRNA was obtained by assessing the effect of MSY2 on stability of a reporter mRNA in mutant oocytes. Based on luciferase activity, the reporter mRNA was less stable in mutant oocytes, and coinjection of a cRNA-encoding wild-type MSY2, but not a cRNA encoding a mutant form unable to bind RNA, substantially restored luciferase activity (Fig. 4A). Increased amounts of reporter mRNA were also present in mutant oocytes following expression of wild-type MSY2 but not mutant MSY2, further strengthening the conclusion that MSY2 binding to RNA confers RNA stability (Fig. 4B).

Onset of Transcriptional Quiescence Is Delayed in Msy2$^{-/-}$ *Oocytes*

A progressive decrease in transcription initiates around midgrowth, the time of antrum formation [21, 22], such that full-grown oocytes are essentially transcriptionally quiescent. Although it is not apparent why transcription ceases prior to completion of growth, it appears to be a universal hallmark because it is observed in oocytes of all species examined to date. Interestingly, disruption of oocyte-somatic cell interactions delays the timing of onset of transcriptional quiescence and compromises oocyte developmental competence [23].

Although the molecular mechanism that underlies transcriptional quiescence is not well understood, it is associated with a change in DNA configuration. Transcriptionally active oocytes display chromatin that is diffusely localized throughout the

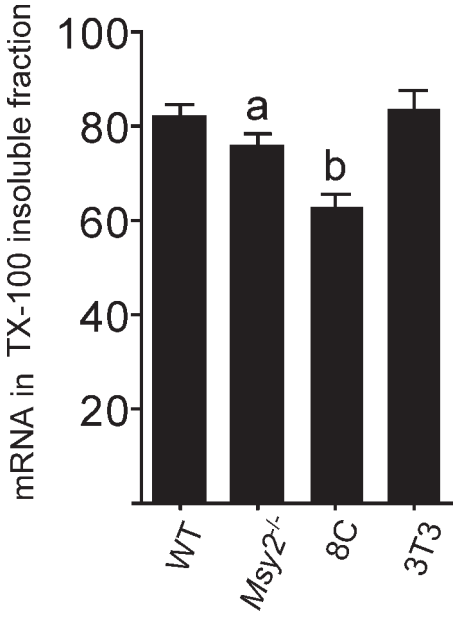

FIG. 3. Relative amount of mRNA in TX-100-insoluble fraction. The total amount of poly(A)-containing RNA was determined in untreated oocytes and in the TX-100-insoluble fraction following treatment, and the data are expressed as the amount in the TX-100-insoluble fraction relative to the total amount. Measurements were made on wild-type (WT) and mutant (*Msy2*$^{-/-}$) oocytes, eight-cell wild-type embryos (8C), and 3T3 cells. The experiment was performed at least seven times for any given sample and the data are expressed as the mean ± SEM; 20 oocytes or embryos in each group were used for each experiment. a, $P < 0.05$, b, $P < 0.0001$.

nucleus, the so-called NSN configuration, whereas in transcriptionally inactive oocytes the chromatin is condensed around the nucleolus, the SN configuration. This association, however, is not causal because oocytes deficient in nucleoplasmin 2 (*Npm2*) do not undergo the NSN to SN change but still become transcriptionally quiescent [24]. Reciprocally, inducing histone hyperacetylation with trichostatin A results in chromatin decondensation in euchromatin regions—centromeric heterochromatin associated with the nucleolus shows only a partial response—without any obvious increase in transcription [25]. Finally, oocytes deficient in MLL2, which is responsible for the bulk of H3K4me3, undergo the NSN to SN transition but are transcriptionally active [26].

We noted that a significantly larger fraction of oocytes obtained from eCG-primed *Msy2*$^{-/-}$ mice were largely devoid of attached cumulus cells when compared to oocytes obtained from wild-type mice (Fig. 5). This lack of firmly adhering cumulus cells led us to examine global transcriptional activity as assayed by BrUTP incorporation and the incidence of the NSN and SN configurations. In contrast to wild-type oocytes that displayed with oocyte development a decrease in the fraction of transcriptionally active oocytes, mutant oocytes remained transcriptionally active (Fig. 6A). The large majority of wild-type oocytes displayed an SN or partial SN (PSN) configuration and were transcriptionally quiescent (SN) or showed a small degree of BrUTP incorporation (PSN), whereas the small portion of NSN wild-type oocytes exhibited readily detectable levels of BrUTP incorporation (Fig. 6B). In marked contrast, only a small fraction of mutant oocytes exhibited the SN configuration and remained transcriptionally active. Almost 90% of mutant oocytes exhibited the NSN configuration and displayed much higher levels of BrUTP incorporation when compared to wild-type oocytes (Fig. 6B). As anticipated, RNA polymerase II bearing a CTD phosphorylated on S5 of the repeat, a marker of RNA polymerase II engaged in initiating transcription [27], was present not only in NSN but not SN wild-type oocytes, but also in mutant oocytes (Fig. 6C).

Changes in histone modifications are linked to changes in gene expression [28, 29], and global changes in histone modifications occur during oocyte growth [30–33]. Accordingly, we used immunocytochemistry to ascertain whether changes in histone modifications associated with either transcription activation or repression were perturbed in mutant oocytes. Although histone H4 acetylation is associated with transcriptionally permissive chromatin, a dramatic decrease in H4 acetylation was observed in mutant oocytes (Fig. 7), as was H3K4me3, which marks active genes [34]. In contrast, there was a marked decrease in marks associated with repression,

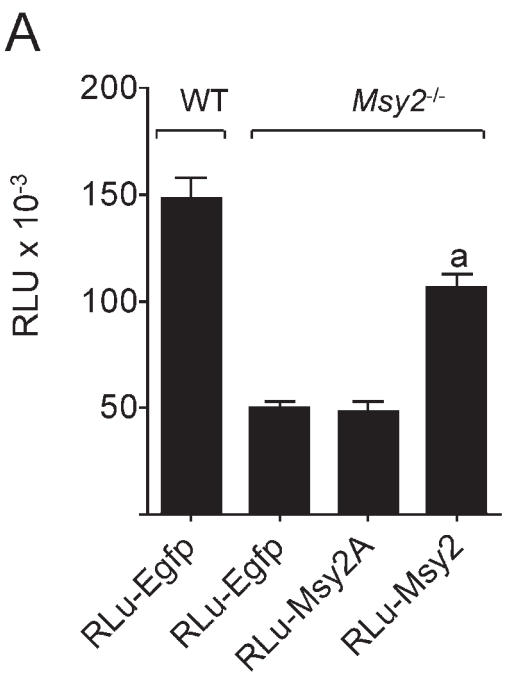

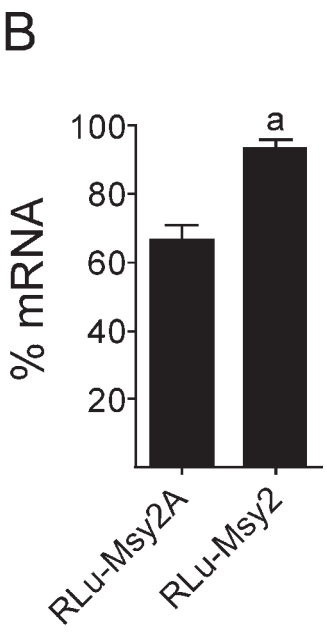

FIG. 4. Messenger RNA stability in *Msy2*$^{-/-}$ oocytes. **A**) Wild-type (WT) or mutant (*Msy2*$^{-/-}$) oocytes were injected with a Luc cRNA. WT oocytes were then subsequently injected with *Egfp* cRNA (RLu-Egfp), whereas mutant oocytes were injected with either an *Egfp* cRNA (RLu-Egfp), a cRNA encoding a mutant form of MSY2 not able to bind to RNA (RLu-Msy2A), or a cRNA encoding WT MSY2 (RLu-Msy2). The oocytes were cultured in the presence of 2.5 μM milrinone to inhibit maturation and after 18 h luciferase activity was measured in individual oocytes. The experiment was conducted three times and the data are expressed as the mean ± SEM. **B**) The experiment was conducted as described in **A** but following culture the amount of *Luc* cRNA in the oocytes (20) was measured by qRT-PCR. The experiment was performed three times and the data are expressed as mean ± SEM. a, $P < 0.0001$.

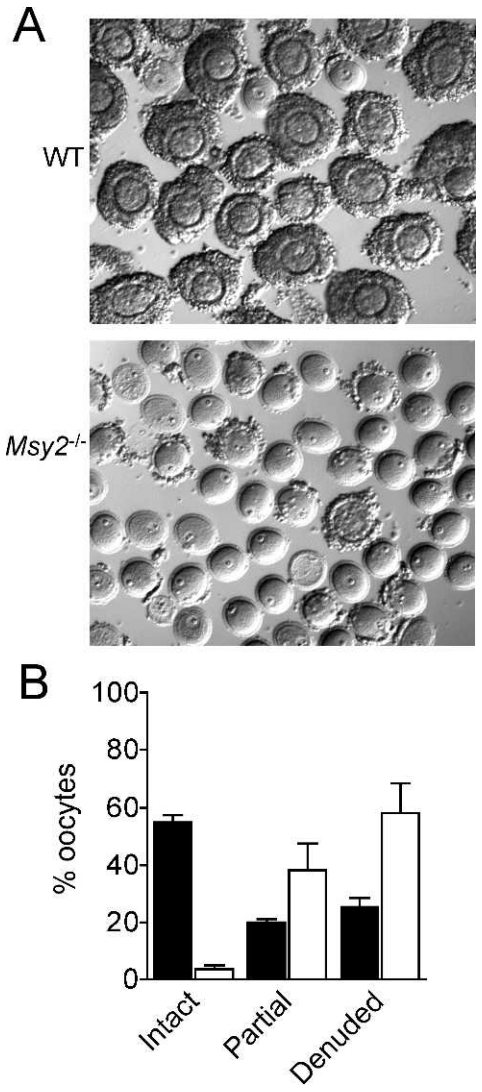

FIG. 5. Loose association of cumulus cells with *Msy2*$^{-/-}$ oocytes. **A**) Photomicrographs of wild-type and mutant oocytes obtained from 22-day mice injected with eCG on day 20. Note compact association of cumulus cells with wild-type oocytes but almost virtual absence of associated cumulus cells with mutant oocytes. Original magnification ×150. **B**) Oocytes were classified as either being intact , i.e., totally surrounded by cumulus cells, partially denuded (partial), i.e., incompletely surrounded by cumulus cells and not exhibiting a tight compactness of the surrounding cumulus cells, or denuded, i.e., essentially free of associated cumulus cells. The experiment was performed five times and the data are expressed as mean ± SEM; between 70 and 130 oocytes were analyzed for each experiment. Solid bars, wild-type oocytes; open bars, *Msy2*$^{-/-}$ oocytes. All of the differences for any category are significant with a P value of at least <0.05.

e.g., H3K9me3 (Fig. 7). These latter changes could account for the continued transcription in mutant oocytes.

Transcript Profiling of Msy2$^{-/-}$ *Oocytes*

To gain further insight in the role of MSY2 in oocyte development, transcript profiling experiments were performed on wild-type and mutant oocytes. As anticipated, the two groups clustered separately (Supplemental Fig. S3). Quantitative RT-PCR (qRT-PCR) was conducted on three transcripts whose relative abundance was increased and three whose relative abundance was decreased in mutant oocytes relative to wild-type oocytes. The microarray data indicated that transcripts for *Hdac1*, *Cdc14b*, and *Eif1a* displayed increases of 3.9-, 3.8-, and 2.3-fold, respectively, and qRT-PCR indicated increases of 4-, 3.7-, and 4-fold, respectively. The microarray data also indicated that transcripts for *Khdrbs1*, *Nfx1*, and *Yy1* displayed decreases of 6.6-, 1.4-, and 2.9-fold, respectively, and qRT-PCR indicated decreases of 2.3-, 1.8-, and 0-fold, respectively. These data lend confidence to interpretations based on the microarray data.

Consistent with a central role for MSY2 in regulating mRNA stability during oocyte growth is the large number of transcripts whose relative abundance was affected in mutant oocytes. Of the 19 548 transcripts detected, the abundance of ~70% in mutant oocytes was affected, with 6940 and 6497 transcripts being either increased or decreased, respectively. Using a 2-fold change as a cutoff, the relative abundance of 3627 and 3357 displayed either an increase or decrease, respectively. A list of transcripts displaying either a 2-fold decrease or increase in relative abundance in mutant oocytes is found in Supplemental Tables S2 and S3, and DAVID analyses are found in Supplemental Tables S4 and S5.

A set of transcripts is degraded during oocyte maturation [35]. These transcripts could be inherently less stable and therefore their abundance may be more affected in the absence of MSY2. Using a 2-fold decrease as a cutoff, of the 3002 transcripts identified by Su et al. [35], 591 were common to the set of 3357 down-regulated transcripts in mutant oocytes, i.e., ~17.5%. Interestingly, of the 1091 transcripts that appear to be inherently unstable in oocytes [36], 41 were down-regulated in mutant oocytes using a 2-fold change as a cutoff, i.e., ~1%. A bioinformatic analysis of the 3′ UTR sequence of transcripts whose relative abundance was reduced in *Msy2*$^{-/-}$ oocytes was uninformative.

DISCUSSION

We report here that depletion of MSY2 in mouse oocytes leads to a plethora of effects that include a reduced growth rate that results in smaller oocytes that do not mature properly, a failure to become transcriptionally quiescent, a decrease in mRNA stability, and a dramatic perturbation of the transcriptome. These effects presumably account for *Msy2*$^{-/-}$ females being infertile.

The rate of oocyte growth during the first wave of folliculogenesis in *Msy2*$^{-/-}$ mice is less than that in wild-type mice and takes an additional 5 days to reach the same diameter as their 22-day-old wild-type counterparts. It should be noted that the cytoplasm of mutant oocytes obtained from 27-day-old mice appears highly granulated, suggesting the cells are or are becoming unhealthy. The slower growth rate of mutant oocytes is consistent with their containing a reduced amount of mRNA, which would presumably support a reduced rate of protein synthesis. The highly compromised ability of mutant oocytes to mature to MII is not a consequence of their slightly smaller size, because oocytes from mice 19 days of age readily mature to and arrest at MII [37]. Rather, their failure to mature properly likely reflects a gross perturbation in their transcriptome.

The ability of mutant oocytes to resume meiosis in the presence of 1 μM milrinone was unanticipated. A possible explanation for this observation is that even though milrinone is a specific inhibitor of PDE3A, which is responsible for eliciting the maturation-associated decrease in cAMP [38], the relative abundance of *Pde10a* transcripts is increased 2.4-fold in mutant oocytes and could in principle promote the maturation-associated decrease in cAMP. In addition, the transcript encoding PDE6D, a cGMP-specific PDE, is up-

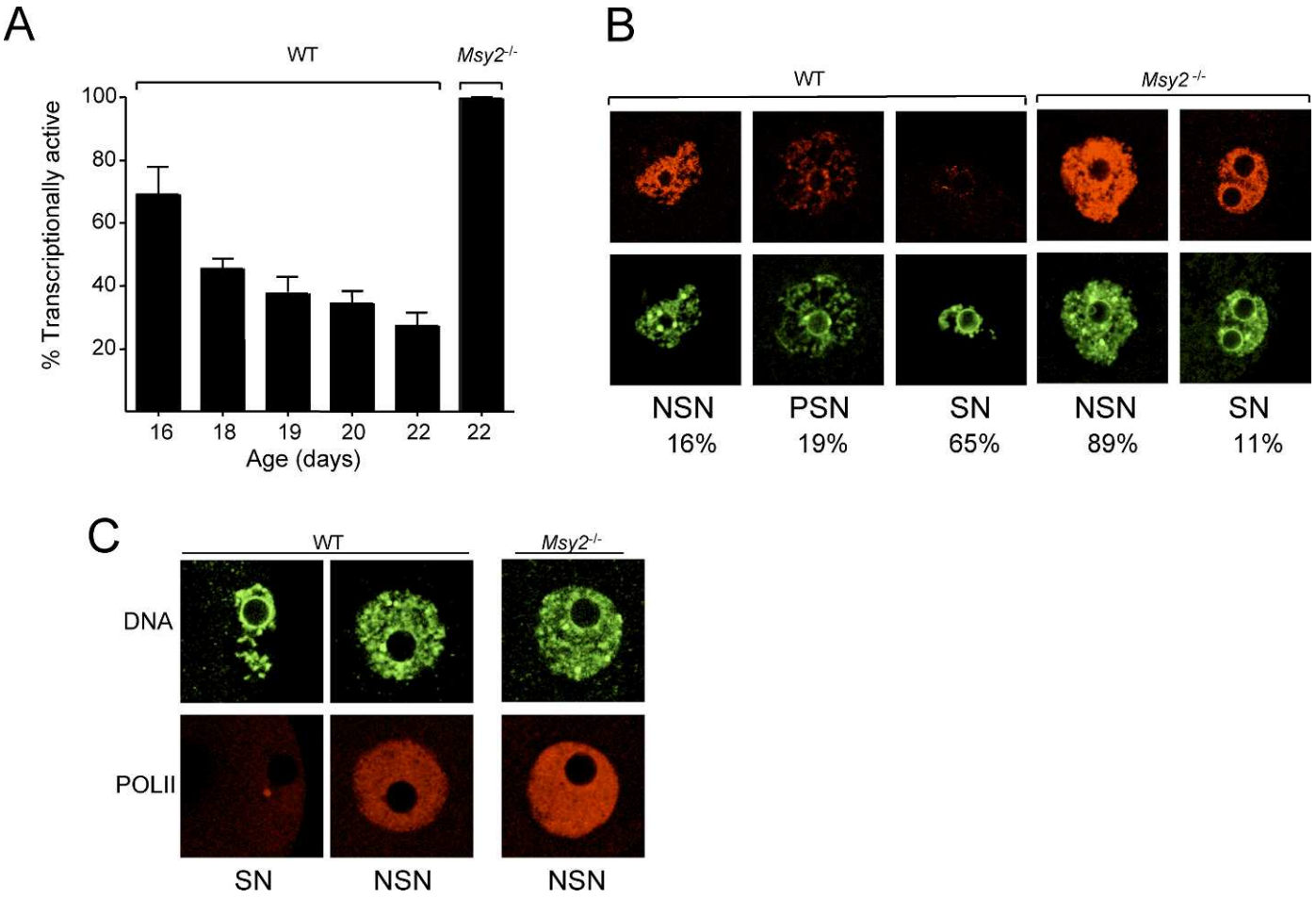

FIG. 6. Transcriptional activity in *Msy2*$^{-/-}$ oocytes. **A**) Transcriptional activity in WT and mutant oocytes was assayed by BrUTP incorporation as a function of mouse age. The experiment was performed three times and the data are expressed as mean ± SEM; at least 25 oocytes were analyzed in each sample. **B**) Representative photomicrographs depicting BrUTP incorporation (red) and DNA staining (green). DNA configuration was classified as NSN, PSN, or SN, and the percentage of the total population distribution is shown below. Note in WT that the transition from NSN to SN is associated with transcriptional quiescence, whereas SN mutant oocytes remain transcriptionally active. **C**) Immunocytochemical detection of active RNA polymerase II (POLII). Original magnification ×400.

regulated 2.4-fold in mutant oocytes; although PDE10A can also hydrolyze cGMP in vitro, whether it can do so in vivo is not known [39]. Recent studies have documented that cGMP serves as a major locus of control of maturation by inhibiting PDE3A [40, 41]; both cGMP and cAMP bind with high affinity to PDE3A, but cGMP is poorly hydrolyzed and thereby serves as a competitive inhibitor [39]. Therefore, an increase in PDE6D activity could result in a decrease in oocyte cGMP, thereby relieving cGMP-mediated inhibition of PDE3A, which may have residual activity in the presence of 1 μM milrinone. Interestingly, there is no indication of precocious maturation when oocytes are isolated from *Msy2*$^{-/-}$ mice, suggesting that in vivo PDE3A is sufficiently inhibited to maintain meiotic arrest.

The bulk of oocyte mRNAs, which are remarkably stable during oocyte growth, is associated with a TX-100-insoluble fraction and with MSY2; RNase treatment releases MSY2 into the soluble fraction [10]. The finding that there is only a very small decrease in the amount of mRNA associated with the TX-100-insoluble fraction in mutant oocytes suggests that MSY2 is not essential to recruit mRNA to this fraction. Consistent with this interpretation is that the bulk of mRNA is associated with a TX-100-insoluble fraction in both eight-cell embryos and 3T3 cells, neither of which contains MSY2. Results of the experiments in which *Luc* mRNA stability was assessed in wild-type and mutant oocytes, coupled with the ability of wild-type MSY2, but not a mutant form unable to bind RNA, to restore *Luc* mRNA stability in mutant oocytes provide additional support that MSY2-binding confers mRNA stability.

The evidence accumulated to date suggests a central role for MSY2 in mRNA stability. Nevertheless, only a modest 25% decrease in the total amount of mRNA is detected in mutant oocytes. One explanation is that mutant oocytes do not become transcriptionally quiescent as do wild-type oocytes during the growth phase. Continuation of transcription could compensate for reduced mRNA stability and thereby result in a less severe decrease in total mRNA. Continued transcription could also account for the increase in transcript abundance of numerous mRNAs in mutant oocytes when compared to wild-type oocytes.

The molecular basis for why mutant oocytes fail to become transcriptionally quiescent is not clear, although the loose association with cumulus cells may be a factor [23]. Changes in histone modifications are a potential mechanism, but the linkage between such changes and establishment of transcriptional quiescence is poor. For example, although oocyte growth is accompanied by cessation of transcription, there is a

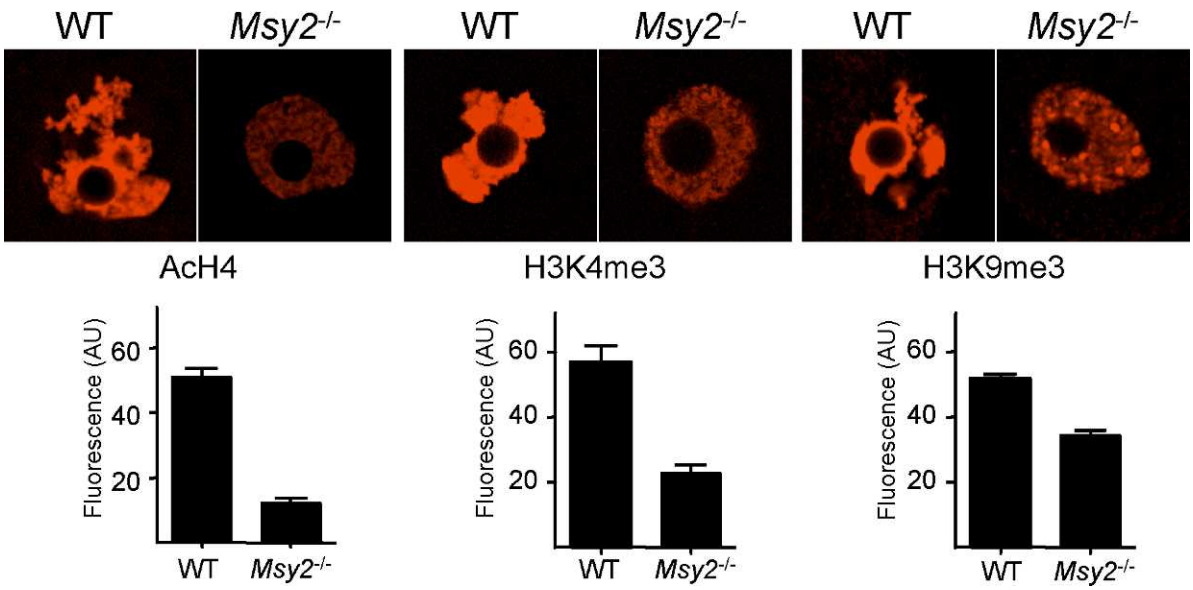

FIG. 7. Histone modifications in $Msy2^{-/-}$ oocytes. Shown are representative photomicrographs of wild-type and mutant oocytes in which acetylated histone H4 (AcH4), histone H3 trimethylated on K4 (H3K4me3), and histone H3 trimethylated on K9 (H3K9me3) was detected by immunocytochemistry. Shown below is the quantification of the fluorescent signal in arbitrary units in which the data are expressed as mean ± SEM; the experiment was performed three times and at least 20 oocytes were analyzed in each group for each experiment. For each histone modification, the differences in signal intensity between wild-type and mutant are significant, $P < 0.0001$. Original magnification ×400.

progressive increase in histone H4 acetylation and histone H3 K4 methylation [31], which are characteristic of transcriptionally permissive chromatin. More striking is a dramatic increase in the extent of H3K9 trimethylation—trimethylated H3K9 is positioned at promoters of repressed genes [34]—that initiates at the onset of the decrease in transcription. This finding suggests that acquisition of repressive histone marks trumps activating marks in directing the overall transcriptional activity of the oocyte. Consistent with this interpretation is that although histone H4 acetylation and H3K4me3 are markedly decreased in mutant oocytes, H3K9me3 is also reduced, which would lead to less repression and therefore maintain transcription.

It is not surprising that the relative abundance of a large number of transcripts is affected in MSY2-deficient oocytes, given the likely role that MSY2 serves as a master regulator of global mRNA stability. Although Selex analysis reveals that the *Xenopus* ortholog FRGY2 can preferentially bind to AACAUC [42], and in male germ cells MSY2, which can also function as a transcription factor, preferentially binds to mRNAs that are transcribed from genes that contain a Y-box DNA-binding consensus sequence in their promoters [43], there is little evidence that MSY2 binds to a specific subset of mRNAs in oocytes. Thus, it is difficult to assess the extent to which changes in transcript abundance in mutant oocytes reflect primary rather than secondary changes. In fact, the relative abundance of transcripts encoding factors involved in transcription is perturbed in mutant oocytes. A decrease in a transcript encoding an activator or repressor of transcription and whose stability is controlled by MSY2 could result in a decreased or increased abundance of target genes, respectively. Such indirect effects are likely. For example, using a 2-fold cutoff, 393 transcripts are misexpressed in $Ctcf^{-/-}$ oocytes [44], of which 117 are common to the set of 6984 misexpressed transcripts in $Msy2^{-/-}$ oocytes, i.e., ~1.5%. *Dicer1* expression is also reduced ~3–4-fold in $Msy2^{-/-}$ oocytes. Again using a 2-fold cutoff, of the 1245 transcripts whose expression is perturbed in $Dicer1^{-/-}$ oocytes, 366 are common to the set of misexpressed transcripts in $Msy2^{-/-}$ oocytes [45], i.e., ~5%. Decreased expression of RNA-binding proteins such as DAZL, whose transcript abundance is reduced ~4-fold in $Msy2^{-/-}$ oocytes, could also lead to changes in abundance of DAZL-binding mRNAs [46].

Bidirectional communication occurs between oocytes and the surrounding granulosa/cumulus cells in which the oocyte drives the conversation [47]. Perturbation of the oocyte transcriptome in $Msy2^{-/-}$ oocytes could disrupt such communication and lead to loss of tight association of cumulus cells with the oocyte. Of interest is that the relative abundance of *Bmp15* transcripts appears overexpressed (2.4-fold) in mutant oocytes (Supplemental Table S3). Whether such misexpression leads to loosely adhering cumulus cells is unknown.

In summary, our previous results [9–11, 13], coupled with the results described here, implicate MSY2 playing a seminal role in regulating mRNA stability in oocytes. During the growth phase, interaction of MSY2 with mRNA confers mRNA stability by a mechanism that, although yet not understood, likely involves shielding the mRNAs from the RNA-degradation machinery. The maturation-associated phosphorylation of MSY2 then initiates the transition to mRNA instability by making mRNAs more susceptible to degradation. Degradation of MSY2, which is essentially complete by the two-cell stage, ensures that the transition from mRNA stability to instability is not only irreversible but also may be critical to execute successfully the maternal-to-embryo transition.

ACKNOWLEDGMENTS

The authors thank Karen Schindler and Paula Stein for critically reading the manuscript.

REFERENCES

1. Schultz RM, Wassarman PM. Biochemical studies of mammalian oogenesis: protein synthesis during oocyte growth and meiotic maturation. J Cell Sci 1977; 24:167–194.
2. Bachvarova R, DeLeon V. Polyadenylated RNA of mouse ova and loss of maternal RNA in early development. Dev Biol 1980; 74:1–8.

3. Brower PT, Gizang E, Boreen SM, Schultz RM. Biochemical studies of mammalian oogenesis: synthesis and stability of various classes of RNA during growth of the mouse oocyte in vitro. Dev Biol 1981; 86:373–383.
4. De Leon V, Johnson A, Bachvarova R. Half-lives and relative amounts of stored and polysomal ribosomes and poly(A) + RNA in mouse oocytes. Dev Biol 1983; 98:400–408.
5. Jahn CL, Baran MM, Bachvarova R. Stability of RNA synthesized by the mouse oocyte during its major growth phase. J Exp Zool 1976; 197:161–171.
6. Paynton BV, Rempel R, Bachvarova R. Changes in state of adenylation and time course of degradation of maternal mRNAs during oocyte maturation and early embryonic development in the mouse. Dev Biol 1988; 129:304–314.
7. Piko L, Clegg KB. Quantitative changes in total RNA, total poly(A), and ribosomes in early mouse embryos. Dev Biol 1982; 89:362–378.
8. Schultz RM. The molecular foundations of the maternal to zygotic transition in the preimplantation embryo. Hum Reprod Update 2002; 8:323–331.
9. Yu J, Hecht NB, Schultz RM. Expression of MSY2 in mouse oocytes and preimplantation embryos. Biol Reprod 2001; 65:1260–1270.
10. Yu J, Hecht NB, Schultz RM. Requirement for RNA-binding activity of MSY2 for cytoplasmic localization and retention in mouse oocytes. Dev Biol 2003; 255:249–262.
11. Yu J, Deng M, Medvedev S, Yang J, Hecht NB, Schultz RM. Transgenic RNAi-mediated reduction of MSY2 in mouse oocytes results in reduced fertility. Dev Biol 2004; 268:195–206.
12. Yang J, Medvedev S, Yu J, Tang LC, Agno JE, Matzuk MM, Schultz RM, Hecht NB. Absence of the DNA-/RNA-binding protein MSY2 results in male and female infertility. Proc Natl Acad Sci U S A 2005; 102:5755–5760.
13. Medvedev S, Yang J, Hecht NB, Schultz RM. CDC2A (CDK1)-mediated phosphorylation of MSY2 triggers maternal mRNA degradation during mouse oocyte maturation. Dev Biol 2008; 321:205–215.
14. Chatot CL, Ziomek CA, Bavister BD, Lewis JL, Torres I. An improved culture medium supports development of random-bred 1-cell mouse embryos in vitro. J Reprod Fertil 1989; 86:679–688.
15. Wiersma A, Hirsch B, Tsafriri A, Hanssen RG, Van de Kant M, Kloosterboer HJ, Conti M, Hsueh AJ. Phosphodiesterase 3 inhibitors suppress oocyte maturation and consequent pregnancy without affecting ovulation and cyclicity in rodents. J Clin Invest 1998; 102:532–537.
16. Kurasawa S, Schultz RM, Kopf GS. Egg-induced modifications of the zona pellucida of mouse eggs: effects of microinjected inositol 1, 4, 5-trisphosphate. Dev Biol 1989; 133:295–304.
17. Aoki F, Worrad DM, Schultz RM. Regulation of transcriptional activity during the first and second cell cycles in the preimplantation mouse embryo. Dev Biol 1997; 181:296–307.
18. Pan H, O'Brien MJ, Wigglesworth K, Eppig JJ, Schultz RM. Transcript profiling during mouse oocyte development and the effect of gonadotropin priming and development in vitro. Dev Biol 2005; 286:493–506.
19. Schultz RM, Montgomery RR, Belanoff JR. Regulation of mouse oocyte maturation: implication of a decrease in oocyte cAMP and protein dephosphorylation in commitment to resume meiosis. Dev Biol 1983; 97:264–273.
20. Bachvarova R, De Leon V, Johnson A, Kaplan G, Paynton BV. Changes in total RNA, polyadenylated RNA, and actin mRNA during meiotic maturation of mouse oocytes. Dev Biol 1985; 108:325–331.
21. Moore GPM. The RNA polymerase activity of the preimplantation mouse embryo. J Embryol Exp Morphol 1975; 34:291–298.
22. Moore GPM, Lintern-Moore S. Transcription of the mouse oocyte genome. Biol Reprod 1978; 17:865–870.
23. De La Fuente R, Eppig JJ. Transcriptional activity of the mouse oocyte genome: companion granulosa cells modulate transcription and chromatin remodeling. Dev Biol 2001; 229:224–236.
24. Burns KH, Viveiros MM, Ren Y, Wang P, DeMayo FJ, Frail DE, Eppig JJ, Matzuk MM. Roles of NPM2 in chromatin and nucleolar organization in oocytes and embryos. Science 2003; 300:633–636.
25. De La Fuente R, Viveiros MM, Burns KH, Adashi EY, Matzuk MM, Eppig JJ. Major chromatin remodeling in the germinal vesicle (GV) of mammalian oocytes is dispensable for global transcriptional silencing but required for centromeric heterochromatin function. Dev Biol 2004; 275:447–458.
26. Andreu-Vieyra CV, Chen R, Agno JE, Glaser S, Anastassiadis K, Stewart AF, Matzuk MM. MLL2 is required in oocytes for bulk histone 3 lysine 4 trimethylation and transcriptional silencing. PLoS Biol 2010; 8.
27. Komarnitsky P, Cho EJ, Buratowski S. Different phosphorylated forms of RNA polymerase II and associated mRNA processing factors during transcription. Genes Dev 2000; 14:2452–2460.
28. Jenuwein T, Allis CD. Translating the histone code. Science 2001; 293:1074–1080.
29. Ruthenburg AJ, Li H, Patel DJ, Allis CD. Multivalent engagement of chromatin modifications by linked binding modules. Nat Rev Mol Cell Biol 2007; 8:983–994.
30. Akiyama T, Kim JM, Nagata M, Aoki F. Regulation of histone acetylation during meiotic maturation in mouse oocytes. Mol Reprod Dev 2004; 69:222–227.
31. Kageyama S, Liu H, Kaneko N, Ooga M, Nagata M, Aoki F. Alterations in epigenetic modifications during oocyte growth in mice. Reproduction 2007; 133:85–94.
32. Liu H, Kim JM, Aoki F. Regulation of histone H3 lysine 9 methylation in oocytes and early pre-implantation embryos. Development 2004; 131:2269–2280.
33. Sarmento OF, Digilio LC, Wang Y, Perlin J, Herr JC, Allis CD, Coonrod SA. Dynamic alterations of specific histone modifications during early murine development. J Cell Sci 2004; 117:4449–4459.
34. Hublitz P, Albert M, Peters AH. Mechanisms of transcriptional repression by histone lysine methylation. Int J Dev Biol 2009; 53:335–354.
35. Su YQ, Sugiura K, Woo Y, Wigglesworth K, Kamdar S, Affourtit J, Eppig JJ. Selective degradation of transcripts during meiotic maturation of mouse oocytes. Dev Biol 2007; 302:104–117.
36. Puschendorf M, Stein P, Oakeley EJ, Schultz RM, Peters AH, Svoboda P. Abundant transcripts from retrotransposons are unstable in fully grown mouse oocytes. Biochem Biophys Res Commun 2006; 347:36–43.
37. Sorensen RA, Wassarman PM. Relationship between growth and meiotic maturation of the mouse oocyte. Dev Biol 1976; 50:531–536.
38. Masciarelli S, Horner K, Liu C, Park SH, Hinckley M, Hockman S, Nedachi T, Jin C, Conti M, Manganiello V. Cyclic nucleotide phosphodiesterase 3A-deficient mice as a model of female infertility. J Clin Invest 2004; 114:196–205.
39. Bender AT, Beavo JA. Cyclic nucleotide phosphodiesterases: molecular regulation to clinical use. Pharmacol Rev 2006; 58:488–520.
40. Norris RP, Ratzan WJ, Freudzon M, Mehlmann LM, Krall J, Movsesian MA, Wang H, Ke H, Nikolaev VO, Jaffe LA. Cyclic GMP from the surrounding somatic cells regulates cyclic AMP and meiosis in the mouse oocyte. Development 2009; 136:1869–1878.
41. Vaccari S, Weeks JL II, Hsieh M, Menniti FS, Conti M. Cyclic GMP signaling is involved in the luteinizing hormone-dependent meiotic maturation of mouse oocytes. Biol Reprod 2009; 81:595–604.
42. Bouvet P, Matsumoto K, Wolffe AP. Sequence-specific RNA recognition by the *Xenopus* Y-box proteins. An essential role for the cold shock domain. J Biol Chem 1995; 270:28297–28303.
43. Yang J, Medvedev S, Reddi PP, Schultz RM, Hecht NB. The DNA/RNA-binding protein MSY2 marks specific transcripts for cytoplasmic storage in mouse male germ cells. Proc Natl Acad Sci U S A 2005; 102:1513–1518.
44. Wan LB, Pan H, Hannenhalli S, Cheng Y, Ma J, Fedoriw A, Lobanenkov V, Latham KE, Schultz RM, Bartolomei MS. Maternal depletion of CTCF reveals multiple functions during oocyte and preimplantation embryo development. Development 2008; 135:2729–2738.
45. Murchison EP, Stein P, Xuan Z, Pan H, Zhang MQ, Schultz RM, Hannon GJ. Critical roles for Dicer in the female germline. Genes Dev 2007; 21:682–693.
46. Chen J, Melton C, Suh N, Oh JS, Horner K, Xie F, Sette C, Blelloch R, Conti M. Genome-wide analysis of translation reveals a critical role for deleted in azoospermia-like (Dazl) at the oocyte-to-zygote transition. Genes Dev; 25:755–766.
47. Su YQ, Sugiura K, Eppig JJ. Mouse oocyte control of granulosa cell development and function: paracrine regulation of cumulus cell metabolism. Semin Reprod Med 2009; 27:32–42.